analytical chemistry

Article

pubs.acs.org/ac

Deep-Sea DuraFET: A Pressure Tolerant pH Sensor Designed for Global Sensor Networks

Kenneth S. Johnson,*[,†] Hans W. Jannasch,[†] Luke J. Coletti,[†] Virginia A. Elrod,[†] Todd R. Martz,[‡] Yuichiro Takeshita,[‡] Robert J. Carlson,[§] and James G. Connery[¶]

[†]Monterey Bay Aquarium Research Institute, 7700 Sandholdt Road, Moss Landing, California 95039, United States

[‡]Scripps Institution of Oceanography, University of California San Diego, 9500 Gilman Drive, La Jolla, California 92093, United States

[§]Honeywell Aerospace, 12001 Highway 55, Plymouth, Minnesota 55441, United States

[¶]215 E. Welsh Road, Maple Glen, Pennsylvania 19002, United States

ABSTRACT: Increasing atmospheric carbon dioxide is driving a long-term decrease in ocean pH which is superimposed on daily to seasonal variability. These changes impact ecosystem processes, and they serve as a record of ecosystem metabolism. However, the temporal variability in pH is observed at only a few locations in the ocean because a ship is required to support pH observations of sufficient precision and accuracy. This paper describes a pressure tolerant Ion Sensitive Field Effect Transistor pH sensor that is based on the Honeywell Durafet ISFET die. When combined with a AgCl pseudoreference sensor that is immersed directly in seawater, the system is capable of operating for years at a time on platforms that cycle from depths of several km to the surface. The paper also describes the calibration scheme developed to allow calibrated pH measurements to be derived from the activity of HCl reported by the sensor system over the range of ocean pressure and temperature. Deployments on vertical profiling platforms enable self-calibration in deep waters where pH values are stable. Measurements with the sensor indicate that it is capable of reporting pH with an accuracy of 0.01 or better on the total proton scale and a precision over multiyear periods of 0.005. This system enables a global ocean observing system for ocean pH.

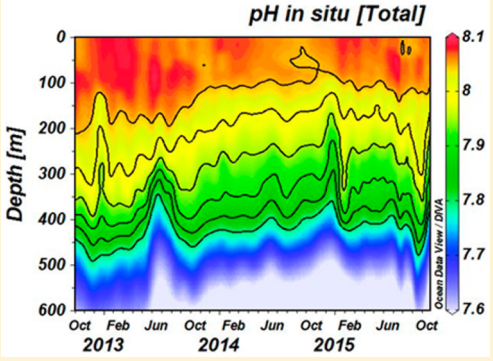

Ocean pH is a dynamic variable that changes on daily, seasonal, interannual, and decadal to centennial time scales. Variability at daily to annual time scales is produced by a variety of processes including photosynthesis, respiration, heating, and ocean physics.[1] The short-term changes are superimposed on a century-scale decrease in surface ocean pH at a rate near −0.002 pH year^{-1}, which is driven by the long-term increase in atmospheric carbon dioxide created by combustion of fossil fuels.[2] This long-term pH decrease, termed ocean acidification, may have profound effects on some organisms. Observations of the annual to weekly scale pH changes provide important constraints on net photosynthesis and respiration in the ocean.

Time series of pH observations with sufficient precision and accuracy to resolve the subannual cycles in the ocean or the long-term trend due to acidification are made at only a handful of sites.[3] These time series are produced by sampling from ships that visit fixed locations at near monthly intervals, followed by sample collection and analysis in laboratories. Such sites are generally near islands with substantial populations that can support a large marine research infrastructure to minimize the extraordinary cost of transits by research vessels to the open ocean. The laboratory pH measurements in these programs are made by spectrophotometry using the indicator dye *m*-cresol purple.[4] The spectrophotometric measurements can be precise and reproducible to 0.002 pH or better.[2,3,5] However, ship-based observations are difficult to achieve with annual or better resolution in most regions of the ocean where long transits by research vessel traveling at typical speeds of 12 knots (22 km h^{-1}) preclude frequent visits. Autonomous sensors that can be deployed in observing systems that are scalable to large numbers are needed.[6]

The requirements for autonomous pH sensors that are designed for large scale observing systems include long-term endurance, precision, and accuracy on the order of a few milli-pH, high reliability, and low cost. Further, such sensor systems should be capable of some form of in situ calibration.[6] Such a reference capability can identify drifting sensor readings and may provide a means to correct for such drift. For example, ocean conditions change much more slowly at depths below 1000 m than at the surface.[2,5,7] Measurements of pH at depths between 1000 and 2000 m serve as an independent check on sensor stability. The ability to measure at depths below 1000 m and near the surface enables much greater reliability in large scale sensor networks by eliminating the need for periodic

Received: December 8, 2015
Accepted: February 18, 2016
Published: February 18, 2016

DOI: 10.1021/acs.analchem.5b04653
Anal. Chem. 2016, 88, 3249−3256

recalibration of the sensors by system operators. Further, pressure tolerant sensors can be parked at great depth, where they avoid most of the impacts of biofouling. This greatly extends their endurance.

There are no instruments generally available that meet these requirements: multiyear endurance, capability of operating through large temperature and pressure ranges, compact size on profiling platforms, and the precision and stability that are required for ocean science applications.[8] Spectrophotometric pH analyzers have exceptional precision and stability[9] but cannot yet meet the power, size, and multiyear endurance requirements of large sensor networks. Potentiometric sensor systems are widely used for in situ studies in freshwater systems.[10] They have sufficiently low power requirements but generally lack the long-term stability needed for remote deployments in the ocean.

The Honeywell Durafet is an Ion Sensitive Field Effect Transistor pH sensor.[11−13] It has been shown to have exceptional stability and accuracy.[12,13] However, the commercially available Durafet package cannot withstand a pressure beyond that equivalent to 70 m depth in the ocean (70 dbar). Further, conventional reference electrodes with liquid junctions are not practical solutions when operated over large pressure and temperature changes.

Here we describe the adaptation of the Durafet ISFET die to operate at pressures equivalent to 2000 m depth in the ocean and the related issue of system calibration to enable accurate pH determinations through large temperature and pressure gradients. We also describe a pressure tolerant, solid-state AgCl reference electrode. The integrated system is termed the "Deep-Sea DuraFET". Operation of the sensor is validated with data collected from a variety of platforms. A particular emphasis for our work is sensor deployment on profiling floats of the type used in the Argo array.[6,14] These floats may have a lifetime in excess of 4 years while profiling from 2000 m to the surface. Nearly 4000 profiling floats are currently operating throughout the ocean. Development of a pH sensor capable of operating for years on these platforms will enable measurements of ocean carbon uptake from the atmosphere and changes in net ocean biological productivity at the global scale with seasonal to annual resolution. Such a capability plays an essential role in validation of global carbon budgets by directly constraining the role of the ocean in the global carbon cycle.

EXPERIMENTAL SECTION

Pressure Tolerant ISFET pH Sensor. The Deep-Sea DuraFET sensor consists of a pH-sensitive ISFET,[11] a AgCl reference electrode, and a titanium counter electrode[15] housed in a pressure tolerant package. The ISFET die is identical to those used in commercially available Durafet pH sensors. The polyether ether ketone (PEEK) housing for the die (Figure 1) is designed to minimize stress on the die while protecting the body of the ISFET from seawater. The die are 3.3 × 4.3 × 0.5 mm with an ∼2 mm ISFET gate centered on the front side. Gold pads on the backside of the die allow for electrical contacts to the Source, Drain, and substrate of the ISFET transistor. The die is held in a pocket in the PEEK housing and secured by a PEEK cover that allows the gate of the ISFET to be exposed to seawater or test solution. The cover is sealed with two 0.5 mm thick Viton-75 O-rings (Figure 1) to prevent incursion of seawater.[16] One O-ring lies on the surface of the die; the second seals the cover to the PEEK housing body (Figure 1). Three 0.25 mm silver wires are epoxied into the

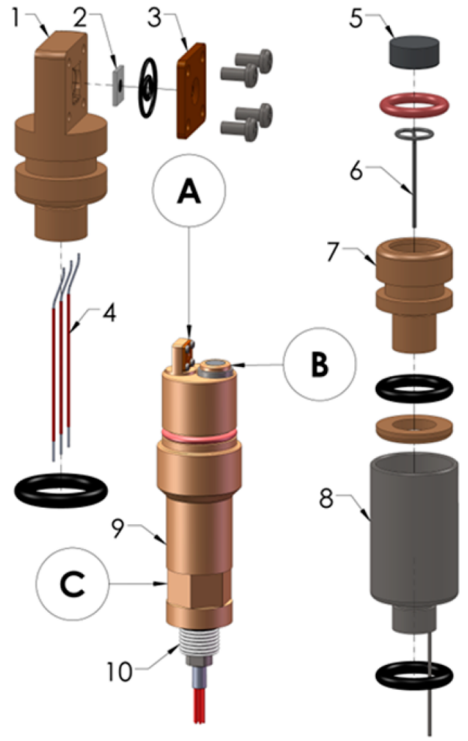

Figure 1. ISFET housing (1) holds the silicon die (2) which is sealed with two O-rings and a cover (3). Three silver wires (4) make contact with gold pads on the back of the die. The AgCl reference pellet (5) and connecting wire (6) are bonded into housing (7) with silver conductive epoxy and then screwed into the Ti counter electrode (8). The assembled ISFET sensor (A) and reference and counter electrodes (B) are then mounted in a PEEK stem (9) which mounts on a pressure housing with a stainless steel connector (10).

PEEK housing and make electrical contacts to the Source, Drain, and substrate gold pads on the back side of the die. The wires are formed so that assembly of the die into the pocket spring-loads the wires. This contact allows continual electrical conductivity during thermal and pressure cycling.

The reference electrode is made from a 7.2 mm diameter × 3.6 mm thick AgCl pellet obtained from the Van London, Co. The pellet is not pure AgCl but appears to contain a significant amount of Ag_2S, which reduces the electrical resistance of the electrode.[17,18] The pellet is mounted in a PEEK housing with a 7.1 × 1.5 mm O-ring around its outer circumference (Figure 1). A silver-filled epoxy is injected behind the AgCl pellet to provide support and to make electrical contact between the pellet and the signal wire. This wire is terminated with a BNC connector at the electronics board. The reference electrode is exposed directly to seawater and uses the chloride ions found in seawater to set the reference potential. The counter electrode[11,15] consists of a machined titanium tube surrounding the reference electrode (Figure 1).

The ISFET die unit and the combined counter and reference electrode unit can be mounted either directly on a pressure housing for use on Conductivity/Temperature/Depth (CTD) profilers lowered from ships and on moorings or in a stem allowing for a single sensor mounting for use on profiling floats. The stem used on floats allows for a secondary pressure seal, which prevents water entry into the main pressure housing of the float in case the sensor develops a leak.

Electronics. The sensor is a P-channel enhancement mode ISFET operating in saturation with a custom, low power

DOI: 10.1021/acs.analchem.5b04653
Anal. Chem. 2016, 88, 3249−3256

controller based on a Honeywell proprietary design. The electronics simultaneously control Drain to Source voltage and current values[11,13] with a counter electrode[15] acting as a pseudogate. In this case, the voltage between the AgCl reference electrode and the FET source (V_{RS}) shows a Nernstian response to the activity of HCl in solution.[13,19] A buffer amplifier with high-input impedance (Maxim MAX406) followed by a unity gain amplifier with "tri-state" output (Linear LTC2050HV) connects the reference electrode to the measurement circuitry. A bipolar 20-bit A/D converter (Cirrus Logic CS5506) is used to digitize the V_{RS} signal with a resolution of ~4 μV. In order to maintain sensor stability and avoid long warm up times, the ISFET bias circuitry is powered from a backup battery when the controller's measurement circuitry is powered off.

Calibration. Sensors are calibrated for response to temperature and pressure in a custom-built, chemically inert PEEK-lined, titanium test chamber with inside dimensions 2.5 cm diameter × 10 cm long. Four ports allow two sensor sets (both ISFET and reference/counter electrode) to be calibrated at a time. The calibration process uses a LabView program to control a Neslab temperature bath over a range from 2 to 40 °C, an ISCO 260D pressure pump (6-210 bar), a precision YSI 4600 thermistor, Omega PX409 pressure sensor, and two ISFET controllers. The temperature and pressure sensors have NIST traceable calibrations. The pressure and temperature calibration procedure uses a 0.01 m HCl solution. Sensors are first run through a break-in cycle to temperature and pressure maxima and then calibrated by cycling through the range of temperatures and pressures that the sensors will experience when deployed on a profiling float.

Once the sensor is fully assembled and connected to the controller that it will be deployed with, a final calibration of the sensor reference potential is done in seawater at room temperature and pressure. After an initial conditioning to seawater, the sensor is plumbed in line with a Sea-Bird Electronics Model 41 CTD sensor with an integral pump that recirculates seawater from a 20 L reservoir. Seawater was obtained from Monterey Bay, California. The pump circulates the seawater for 8 s with a flow rate of 500 mL min^{-1} at 2 min intervals. The sensor output and other ancillary values are recorded at the end of each interval. No effort is made to regulate the seawater temperature or pH at a fixed value. A CTD measurement is made just prior to the DuraFET readings to record solution temperature and salinity. To assess the seawater pH, a sample of the seawater recirculating through the system is periodically withdrawn, and pH is determined at 20 °C by spectrophotometry.

Spectrophotometric pH. Laboratory pH measurements in seawater used for the final pH sensor calibration were made using a modification of the *m*-cresol purple technique[4] adapted to a 1 cm path length with temperature controlled at 20 °C. Perturbation of seawater pH by the dye is accounted for using the method of standard additions. The mean precision (1SD) was 0.0027 for 36 sets of replicate analyses. Analysis of calibrated tris(hydroxymethyl)aminomethane buffers in artificial seawater provided by A. Dickson (Scripps Institution of Oceanography) gave pH values with absolute offsets from the reported pH < 0.01.

At sea, the pH was measured spectrophotometrically at 20 °C using a custom automated system[20] with *m*-cresol purple without further purification (ACROS Lot A0264321). Water samples for pH measurements were collected from a rosette sampler following standard operating protocols.[21] The precision and accuracy of pH measurements were estimated to be ±0.0015 (duplicate n = 86, 1 SD) and 0.01, respectively. Dissolved inorganic carbon in samples collected at sea was determined using a custom system with an infrared detector (LiCOR 7000).[22]

RESULTS AND DISCUSSION

Industrial applications of ISFET sensors generally use a mechanical seal with elastomer gaskets.[23] We adopted a modification of this system. In our approach, the ISFET die is housed within a machined PEEK assembly and is sealed with O-rings.[16] The assembly is shown in Figure 1. This assembly has been tested to pressures as high as 3000 dbar and pressure cycled over 700 times to 2000 dbar. With the pressure capable design, the challenge is then to calibrate the system at high pressure and various temperatures.

Calibration of Temperature and Pressure Response. When operated in the constant current mode, the voltage between the reference electrode and source of the ISFET sensor (V_{RS}) will exhibit a near Nernstian response if the buffer capacity on the insulator over the gate is high enough.[19] With a AgCl reference electrode, the sensor will then respond directly to the activity of HCl in solution. The response of the Honeywell Durafet and AgCl reference electrode is, in fact, indistinguishable from that expected for the Nernst equation in solutions with pH values from 2 to 10.[24] Further, the sensor is known to have a linear response to temperature.[13] In that case, the Nernst equation for sensor response at temperature T/K and pressure P/bar can be written as

$$\begin{aligned} V_{RS} &= k_0 + k_2(T - 273.15) + f(P) - \frac{RT}{F}\ln(10)\log(a_H a_{Cl})_{T,P} \\ &= k_0 + k_2(T - 273.15) + f(P) - \frac{RT}{F}\ln(10)[\log(m_{H,F} m_{Cl}) \\ &\quad + \log(\gamma_H \gamma_{Cl})_{T,1}] - \bar{V}_{HCl}\frac{P}{F} \end{aligned} \quad (1)$$

k_0 is the standard potential of a conventional electrochemical cell where activities are in their standard state or activities are at unit value. The standard potential EMF of such a cell is reported at a specified temperature such as 0 °C. k_2 is the temperature dependence of k_0. Unlike the conventional electrochemical cell, ISFET k_0 and k_2 values contain terms associated with FET design, semiconductor processing, and power application values. These extra terms numerically alter k_0 and k_2 values of individual die, but the resulting effect is exceptionally stable. k_0 and k_2 will vary from device to device so each die will have its own unique pair of values determined by test. So as not to imply k_0 and k_2 are single constants for all die, k_0 will be referred to as the "reference potential" and k_2 as its temperature coefficient. f(P) is the pressure coefficient of the sensor. The activity, activity coefficient, and molality of ions are represented by a, γ, and m at the subscripted temperature and pressure (bar). The subscript F on the proton concentration refers to the free proton concentration, which is presumed to be the protons not complexed by sulfate or fluoride ions. The partial molal volume of HCl in solution is given by $\bar{V}_{HCl}$, and P is pressure. R is the universal gas constant, and F is the Faraday constant.

The sensor requires calibration for both its pressure and temperature coefficients before use in the ocean. This can be done by measuring V_{RS} in any solution with known $a_H a_{Cl}$ as a function of pressure and temperature. Practically, the only

DOI: 10.1021/acs.analchem.5b04653
Anal. Chem. 2016, 88, 3249−3256

solutions that readily meet this criteria are dilute solutions of HCl. We have calibrated our sensors in 0.01 m HCl solutions held in the high pressure chamber. The units holding the ISFET and the reference electrode/counter electrode were sealed into the chamber, and the sensors were cycled under computer control from 5 to 40 °C and 0 to 207 bar. The temperature coefficient was computed as the linear slope at constant pressure of the function

$$k_0 + k_2(T - 273.15) = V_{RS} + \frac{RT}{F}\ln(10)[\log(m_{H,F}m_{Cl}) + \log(\gamma_H\gamma_{Cl})_{T,1}] + \overline{V}_{HCl}\frac{P}{F} \quad (2)$$

which was obtained by rearranging eq 1.

The activity coefficients of HCl at various temperatures and 1 bar pressure in 0.01 m HCl were obtained from Harned and Ehlers.[25] The partial molal volume of HCl in pure water was taken from Millero.[26] The results for one experiment at pressures from 50 to 2000 dbar are shown in Figure 2. The offsets between each line are a result of neglecting f(P) in eq 2. The slopes determined from eq 2 are, within the precision we require, independent of pressure.

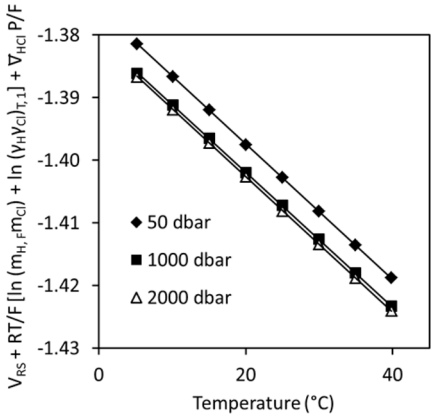

Figure 2. Results from a typical calibration of the temperature coefficient derived from eq 2 at 3 pressures from 50 to 2000 dbar pressure. The mean value of k_2 determined at 21 discrete pressures from 0 to 2100 dbar is −0.001 077 ± 0.000 002 V °C^{-1} (1 SD). Measurements were made in 0.01 m HCl.

The values of f(P) can be determined by rearranging eq 1 and substituting the measured k_2 value

$$f(P) + k_0 = V_{RS} + \frac{RT}{F}\ln(10)[\log(m_{H,F}m_{Cl}) + \log(\gamma_H\gamma_{Cl})_{T,1}] + \overline{V}_{HCl}\frac{P}{F} - k_2(T - 273.15) \quad (3)$$

A plot of the right-hand side of eq 3 versus pressure (Figure 3a) shows f(P) + k_0 for the same experiment shown in Figure 2. A complex shape results, and the shape is different for each sensor. The variation in the sensor potential with pressure results because the Si substrate of the transistor is piezoresistive. Pressure induced strains alter the properties of the transistor. The transistor mounting on a plastic substrate allows multiple bending moments that produce the complex behavior. We have chosen to express f(P) as a sixth order polynomial in pressure to allow for the complexity. The value of f(P) has no significant (relative to the calculation of pH) temperature coefficient, and we express f(P) as a function of pressure only. Each device has a different k_2 and f(P), and they must be individually calibrated.

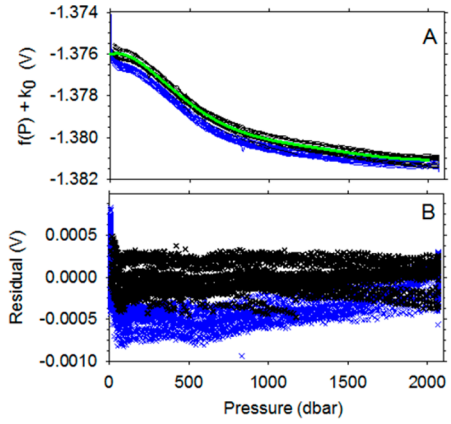

Figure 3. A) Pressure calibration in 0.01 m HCl at temperatures from 5 to 40 °C over the period 13 Dec. 2014 to 19 Dec. 2014 showing data on decompression (black) and compression (blue). The green line is the f(P) + k_0 function fitted to the data on decompression. B) Residuals from f(P) + k_0 function on decompression (black) and compression (blue).

Typical for all of the devices that we have built, the pressure calibration (Figure 3) shows a small amount of hysteresis. The mean offset between f(P) values on compression and the function fitted to values on decompression cycles is about 0.5 mV at maximum (Figure 3b). This likely is produced by insufficient rigidity in the PEEK substrate that supports the ISFET die.

Calibration of Reference Potential. The reference potential k_0 can be determined in any solution with a known activity of HCl. One estimate of the sensor reference potential is obtained during calibration of the temperature and pressure coefficients in 0.01 m HCl. However, the proton concentration in the HCl solution is some 6 orders of magnitude different than that found in seawater. Any error in electrode slope or in the linearity of the electronics would produce much larger errors in proton concentration when sample conditions are far from the calibration conditions. Our preference, therefore, is to calibrate the sensor in a natural seawater sample whose pH has been determined using spectrophotometric methods. The activity of HCl can be obtained from the measured pH, the chloride ion concentration that is known from the salinity,[21] the partial molal volume of HCl in seawater,[26] and the published activity coefficient of HCl in seawater.[27] The volume of seawater should be large enough (order of 10 L) to minimize the rate of pH change due to equilibration with the atmosphere.

Calibration of the sensor requires careful attention to the varied pH and concentration scales that are used in the ocean sciences.[28] The sensor inherently reports the free proton molality, while spectrophotometric pH measurements are calibrated on the total proton scale, which is the concentration of free protons plus HSO_4^-. Further, spectrophotometric measurements are reported as mole per kg seawater. These two scales are related[28] by the following equation

$$[H^+]_T = [H^+]_F + [HSO_4^-] = m_{H,F}\frac{1000}{(1000 - 1.005 \times \text{Salt})} + [HSO_4^-] \quad (4)$$

where brackets denote a concentration in units of mol kg seawater^{-1}, and Salt is seawater salinity measured on the practical salinity scale.[29] The equilibrium constant for

DOI: 10.1021/acs.analchem.5b04653
Anal. Chem. 2016, 88, 3249−3256

dissociation of HSO_4^-, measured on the mole per kg seawater concentration scale,[30] is

$$K_{HSO_4} = \frac{[H^+]_F[SO_4^{2-}]}{[HSO_4^-]} \quad (5)$$

where $[SO_4^{2-}]$ is the sulfate concentration (mol kg seawater^{-1}) in seawater, which is related to the total sulfate, S_T, by[21]

$$S_T = [SO_4^{2-}] + [HSO_4^-] = 8.067 \times 10^{-4} \times \text{Salt} \quad (6)$$

Combining eq 4 and 5 yields

$$[H^+]_T = m_{H,F}\frac{1000}{(1000 - 1.005S)}\left(1 + \frac{[SO_4^{2-}]}{K_{HSO_4}}\right) \approx m_{H,F}\frac{1000}{(1000 - 1.005S)}\left(1 + \frac{S_T}{K_{HSO_4}}\right) \quad (7)$$

Inverting eq 7 allows the value of $m_{H,F}$ that is required for the k_0 calibration to be obtained from the spectrophotometric pH value. There are often small temperature differences (<1 °C) between the spectrophotometric and Deep-Sea DuraFET pH measurements. We use a generic correction[31] for seawater to adjust the spectrophotometric measurements to the temperature at the sensor

$$\frac{\partial \text{pH}_T}{\partial T} = -0.01582°\text{K}^{-1} \quad (8)$$

The activity coefficients of HCl in seawater, which are required in eq 1, come from measurements in artificial seawater.[27] Procedures to compare laboratory and sensor pH in the ocean, with large temperature and pressure variations, are discussed below.

Prior to the calibration in seawater, sensors have only been exposed to 0.01 m HCl. There is sufficient dissolved bromide ion present (~840 μmol kg^{-1}) to form a $AgCl_{1-X}Br_X$ solid solution when the AgCl reference sensor is initially placed in seawater. This may shift the reference potential of the sensor by 2 to 5 mV.[24] The size of the offset appears to be related to composition and construction of the reference electrode. The final calibration should only be carried out after immersing the sensor in seawater for several days to weeks. We prefer to initially expose the sensors to fresh, running seawater to make certain that bromide is not depleted from the recirculated solution.

Samples were collected from the recirculation system at 6 to 36 h intervals during k_0 calibration, and pH was immediately analyzed by spectrophotometry. A least-squares line was fitted to the laboratory pH values (total proton scale) versus time when a smooth pH trend versus time was established. The pH values at the sensor were then estimated at the time of each sensor measurement by converting values predicted from the least-squares fitted line to the in situ temperature with eq 8. These values are plotted as a line labeled Solution_pH in Figure 4. A k_0 value is computed for each observation by converting the Solution_pH to $m_{H,F}$ at the in situ temperature and inserting that value into eq 2 with the k_2 value already determined for the sensor. During this period, the sensor k_0 value may drift as the sensor warms up and final equilibration with Br^- occurs. The recorded data may also undergo offsets as the system is purged of air bubbles. A calibration is complete when the k_0 value is constant to within 0.1 mV for 1 day. When

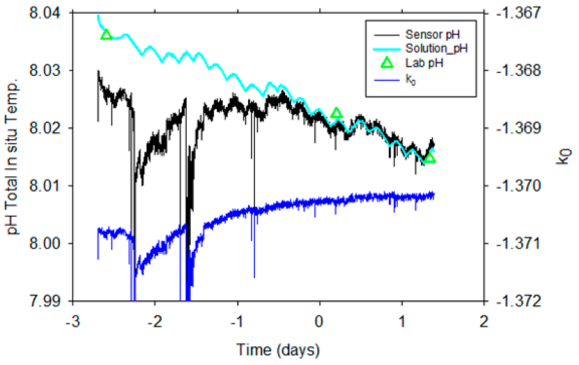

Figure 4. Sensor k_0 calibration data in seawater with salinity 34.5. Temperature varied between 19 and 20 °C during the calibration.

the sensor pH is computed with this final k_0, the sensor pH and Solution_pH will agree to within 0.002 pH for one full day (Figure 4). The final k_0 value is the mean of the last 1 day of measurements, which is −1.370 52 ± 0.000 05 (1 SD) V for the sensor shown in Figure 4.

The degree of agreement between the k_0 values determined in HCl and in seawater is one additional assessment of the Nernstian response of the sensor. Figure 5 shows a comparison

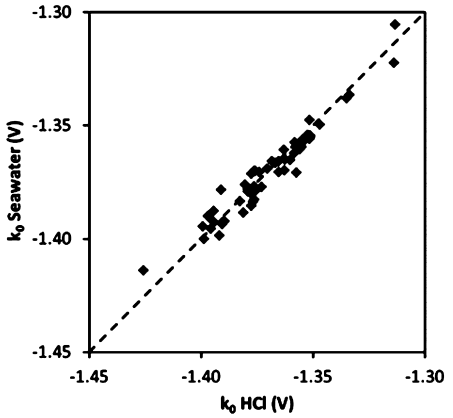

Figure 5. Reference potential (k_0) determined in seawater versus values determined in 0.01 m HCl for 56 different sensors. The dashed line is the 1:1 relationship.

of the k_0 values for a series of 56 sensors that have been assembled and calibrated over the past two years. The pairs of k_0 values cluster closely around a line with a 1:1 slope. The mean difference in k_0 values is 0.001 ± 0.005 V (1 SD). We do not expect exact agreement between the values because a dedicated set of electronics was used in the pressure/temperature calibration system, while the sensors were paired with their deployment electronics for the k_0 calibration in seawater. Within the scatter caused by changing electronics, the two k_0 values agree over 6 orders of magnitude change in proton concentration and nearly 2 orders of magnitude change in chloride concentration. We are, therefore, confident that these sensors show a Nernstian response to both protons and chloride ion, as previously found.[24] As a result, the sensor will operate throughout the open ocean, as well as the large range of salinity found in estuaries,[1] with the limit being the point where chloride ion concentration deviates from a constant ratio to salinity.

DOI: 10.1021/acs.analchem.5b04653
Anal. Chem. 2016, 88, 3249−3256

Ocean Deployments. Deep-Sea DuraFETs have operated at depths up to 3000 m (~3000 dbar) during a variety of deployments in the ocean, and discrete samples have been collected to assess sensor performance. pH in the samples was measured by spectrophotometry on board ship. Dissolved inorganic carbon was determined on separate samples. A direct comparison of the laboratory pH values with the sensor measurements at high pressure and low temperature requires the determination of total dissolved inorganic carbon (C_T) and total alkalinity (A_T) in the discrete samples. These latter two quantities are pressure and temperature independent. In situ pH can be computed from C_T and A_T using an understanding of the pressure and temperature dependence of the equilibrium constants for the first and second dissociation reactions of carbonic acid (K_1 and K_2), boric acid (K_B), and bisulfate (K_{HSO_4}) in seawater.[31,21] In our work, the laboratory pH is combined with measured total dissolved inorganic carbon to estimate the total alkalinity[21] and the in situ pH.

The calibration procedure that has been used with the sensors allows them to produce measurements of $m_{H,F}$ and pH on the free proton scale at the in situ temperature and pressure that are essentially independent of the existing thermodynamics used to study the carbon system in seawater. The two points of intersection with existing carbon system thermodynamics are the use of spectrophotometric pH measurements to determine the sensor k_0 and the dissociation constant of bisulfate that is needed in eq 7 to compare sensor values to the pH values on the total proton scale estimated from laboratory measurements.

Unfortunately, there are several gaps in our knowledge of the thermodynamics used to convert the laboratory pH values to values at high pressure. The dissociation constant of bisulfate in seawater needed to convert between the free proton scale and total proton scale is poorly constrained by experimental procedures,[30] and there is a large range in the reported values.[32] Further, the pressure dependence of the bisulfate dissociation constant in seawater has never been measured. The tabulated values[31] are estimates derived from measurements in water and corrected to seawater media assuming that the effect of seawater media on the molal volume of HSO_4^- is the same as for HCO_3^-.[26] Given the range of effects of seawater on the molal volume of other univalent anions, the uncertainty can translate to a 0.01 pH error at 2000 dbar pressure in pH on the total scale. In addition, the pressure dependence (partial molal volumes) of the dissociation constants of carbon dioxide, bicarbonate, and boric acid are derived from the work of Culberson and Pytkowicz,[33] which was based on an obsolete set of equilibrium constants.

As a result, the pH values extrapolated from laboratory measurements to high pressure have biases on the order of 0.02 pH at pressures near 2000 dbar, based on propagation of possible errors. Such biases are not present in the sensor data, which are derived from an independent thermodynamic framework. In the following comparisons of sensor data and in situ pH estimated from laboratory measurements, we are using the conventional computational scheme in the program CO2Sys,[34] but we recognize that exact correspondences should not be expected.

Initial tests of the calibrated Deep-Sea DuraFET were made on a cruise of the Research Vessel Melville off the Southern California coast in July and December, 2012. A series of 18 and 8 profiles were done on the two cruises to 1000 m depth with a Deep-Sea DuraFET sensor mounted on a 24-place rosette sampler that was equipped with a Sea-Bird Electronics 911 CTD. The sensor was plumbed into the CTD flow stream. Figure 6a shows one of the vertical profiles of pH determined with the Deep-Sea DuraFET and the corresponding pH values estimated at in situ conditions from laboratory measurements. Figure 6b shows the anomalies between these values as a function of pressure for all 26 stations (383 discrete pH measurements) that were sampled on the cruises. The mean difference for all observations is 0.00 ± 0.019 (1 SD), whereas the agreement improves to 0.00 ± 0.011 for all samples below 50 m. The mismatches appear to increase slightly to values near 0.01 at 1000 m, consistent with the gaps in our understanding of the seawater−carbon system at higher pressure. The larger scatter nearest the surface is most likely due to steeper vertical pH gradients that can produce larger mismatches in the water sampled by sensor and bottles.

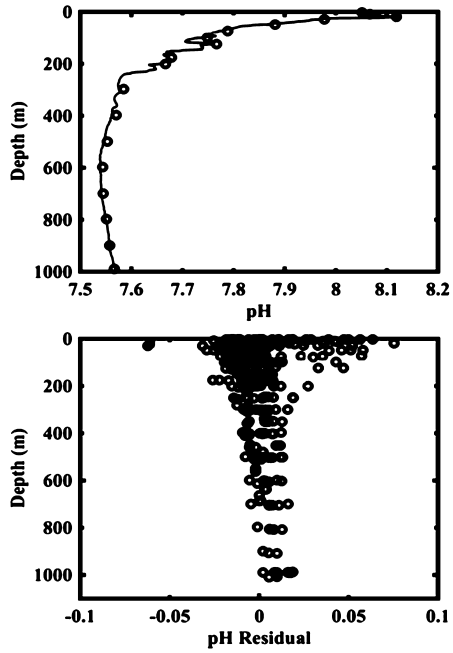

Figure 6. pH profile from the Deep-Sea-DuraFET (black line) and discrete samples measured using spectrophotometry (open circles) is shown on the left. The residual between sensor and discrete samples (n = 383) is shown on the right. The profile was collected at 32.779°N, 117.678°W, 6 July 2012.

Scientific interest in pH is generally greatest for measurements in the upper 1 km of the water column, where anthropogenic carbon dioxide enters the ocean, and where upwelling of carbon dioxide rich, low pH deep waters can influence ecosystem processes.[35] However, if measurements are made only at the surface, it can be difficult to separate sensor drift from oceanographic processes.[36] The capability of the Deep-Sea DuraFET to make measurements through a range of pressures allows deep water with stable pH values[2] to be used as a reference that enables sensor drift to be identified and corrected. To demonstrate this capability, we examine data from Deep-Sea DuraFET pH sensors that were adapted to operate on Teledyne/Webb Research APEX profiling floats.[14,37] These floats have the capability to make about ~280 vertical profiles from depths near 2000 m to the surface. This equates to a 3.5 year lifetime at a 5 day interval between profiles and 7 years at 10 days.

DOI: 10.1021/acs.analchem.5b04653
Anal. Chem. 2016, 88, 3249−3256

We have now deployed nearly 20 profiling floats equipped with pH sensors. The mean rate of drift, diagnosed as the change between pH observed below 1000 m depth and the expected pH at this depth, is −0.036 pH year^{-1}. This drift rate appears to result from insufficient conditioning of these sensors to the bromide found in seawater, as sensors that received extensive exposure to seawater before deployment have near zero drift rates. The drift in sensors that appear poorly conditioned before deployment would render the data returned by these floats unsuitable for some purposes, such as direct detection of acidification rates, if it could not be corrected. The measurements at depths below 1000 m allow a robust correction to be made.

Figure 7 shows the in situ pH values observed at 1200 m depth and at the surface for profiling float 8486 (World Meteorological Organization # 5904124), which profiled from maximum depths near 1400 m. This float was deployed at the Hawaii Ocean Time-series (HOT) station[2] in May 2013 and data is shown through September 2015. The expected pH at 1200 m was determined using a multiple linear regression (MLR) equation that predicts in situ pH values using oxygen, salinity, temperature, and depth as described previously.[38] The MLR was computed from in situ pH derived using C_T and A_T measured at all stations in the Pacifica database[39] between 55°N to 55°S and depths from 500 to 2000 m. The MLR equation fits in situ pH values computed from laboratory pH and A_T data reported by the HOT program and which were not included in the Pacifica database, with a root-mean-square error of 0.01.

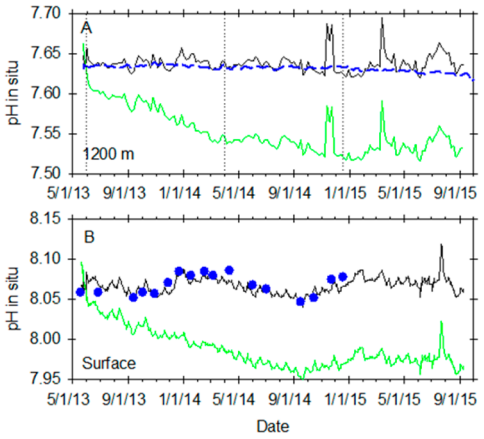

Figure 7. Raw (green) and corrected pH (black) pH values at in situ temperature and pressure on the total proton scale measured by float 8486 near the Hawaii Ocean Time-series station. A) pH values at 1200 m depth. The dashed blue line shows the pH prediction from the MLR that is used to define the deep pH reference value. Vertical dotted lines define periods where linear equations were fitted to the raw data and the difference between these equations and the reference value was used to determine the error in the sensor reference potential k_0. B) pH values at depths <10 m. The blue circles show the surface pH measurements reported by the HOT program, after adjustment to in situ temperature.

The pH reported by float 8486 at 1200 m drifts away from these reference values at a mean rate of −0.08 pH year^{-1} during the first year of deployment (Figure 7a), before the values stabilize. This drift rate is one of the highest values we have observed. We presume that this drift occurs as a change in the sensor reference potential, k_0, with a mean of −0.0044 V year^{-1} in the first year. Producing a corrected pH profile involves first determining a modified k_0 value by adjusting the reference potential so the sensor reproduces the 1200 m pH trend predicted from the MLR equation. This was done by breaking the 1200 m sensor record into 4 segments and fitting each with a linear rate of change in k_0. A corrected pH profile is then computed with the adjusted k_0 value corresponding to the profile date. To assess the accuracy of the adjusted data, we compare the derived pH values in the upper 10 m of the water column with values measured at the same depth by the HOT program (Figure 7b). The average deviation of the adjusted float data from the 17 contemporaneous measurements of surface pH at HOT is 0.004 ± 0.007 (1 SD) with no significant trend in the anomaly over 19 months.

These results demonstrate that, even in one of the worst cases of sensor drift, the measurements can be corrected to a consistency with laboratory measurements of about 0.005 pH in surface waters. This is equivalent to measuring proton concentration at the nanomolar level to within 1% for time periods in excess of one year. This would meet the most stringent requirements that have been outlined for ocean pH observations.[40] Thus, it is feasible to build a global pH observing systems that is capable of assessing the impacts of increasing atmospheric carbon dioxide on the pH of natural waters. Further, recent deployments with sensors that have been much more rigorously conditioned to seawater bromide show far smaller drift rates, and this will enable ever smaller impacts to be observed.

AUTHOR INFORMATION

Corresponding Author

*Phone: 1-831-775-1985. Fax: 1-831-775-1620. E-mail: johnson@mbari.org.

Notes

The authors declare the following competing financial interest(s): The Monterey Bay Aquarium Research Institute, Scripps Institution of Oceanography, and Honeywell International have licensed the Deep-Sea DuraFET for production and sale by Sea-Bird Scientific.

ACKNOWLEDGMENTS

This work was supported by the US National Oceanographic Partnership Program award N00014-10-1-0206 and by the David and Lucile Packard Foundation. The research cruises were funded by the UC Ship Funds Program. We thank Carole Sakamoto and Josh Plant for assistance in the laboratory, the Hawaii Ocean Time-series personnel for deploying profiling floats and providing ready access to their data, and the Captain and crew of the Research Vessel Melville.

REFERENCES

(1) Hofmann, G. E.; Smith, J. E.; Johnson, K. S.; Send, U.; Levin, L. A.; Micheli, F.; Paytan, A.; Price, N. N.; Peterson, B.; Takeshita, Y.; Matson, P. G.; Crook, E. D.; Kroeker, K. J.; Gambi, M. C.; Rivest, E. B.; Frieder, C. a.; Yu, P. C.; Martz, T. R. *PLoS One* **2011**, *6*, e28983.

(2) Dore, J. E.; Lukas, R.; Sadler, D. W.; Church, M. J.; Karl, D. M. *Proc. Natl. Acad. Sci. U. S. A.* **2009**, *106*, 12,35−12240.

(3) Bates, N.; Astor, Y.; Church, M.; Currie, K.; Dore, J.; González-Dávila, M.; Lorenzoni, L.; Muller-Karger, F.; Olafsson, J.; Santa-Casiano, M. A. *Oceanography* **2014**, *27*, 126−141.

(4) Clayton, T. D.; Byrne, R. H. *Deep Sea Res., Part I* **1993**, *40*, 2115−2129.

DOI: 10.1021/acs.analchem.5b04653
Anal. Chem. 2016, 88, 3249−3256

(5) Byrne, R. H.; Mecking, S.; Feely, R. A.; Liu, X. *Geophys. Res. Lett.* **2010**, *37*, L02601.
(6) Johnson, K. S.; Needoba, J. A.; Riser, S. C.; Showers, W. J. *Chem. Rev.* **2007**, *107*, 623−640.
(7) Rios, A. F.; Resplandy, L.; Garcia-Ibanez, M. I.; Fajar, N. M.; Velo, A.; Padin, X. A.; Wanninkhof, R.; Steinfeldt, R.; Rosón, G.; Perez, F. F. *Proc. Natl. Acad. Sci. U. S. A.* **2015**, *112*, 9950−9955.
(8) Martz, T. R.; Daly, K. L.; Byrne, R. H.; Stillman, J. H.; Turk, D. *Oceanography* **2015**, *28*, 40−47.
(9) Martz, T. R.; Carr, J. J.; French, C. R.; Degrandpre, M. D. *Anal. Chem.* **2003**, *75*, 1844−1850.
(10) Pankratova, N.; Crespo, G. A.; Afshar, M. G.; Crespi, M. C.; Jeanneret, S.; Cherubini, T.; Tercier-Waber, M.-L.; Pomati, F.; Bakker, E. *Environ. Sci.: Processes Impacts* **2015**, *17*, 906−914.
(11) Connery, J. G.; Baxter, R. D.; Gulczynski, C. W. *Pittsburgh Conference* **1992**, 1−4.
(12) Sandifer, J. R.; Voycheck, J. J. *Microchim. Acta* **1999**, *131*, 91−98.
(13) Martz, T. R.; Connery, J. G.; Johnson, K. S. *Limnol. Oceanogr.: Methods* **2010**, *8*, 172−184.
(14) Roemmich, D.; Johnson, G. C.; Riser, S.; Davis, R.; Gilson, J.; Owens, W. B.; Garzoli, S.; Schmid, C.; Ignaszewski, M. *Oceanography* **2009**, *22*, 34−43.
(15) Connery, J. G.; Ambler, E. W.; Shaffer, L., Jr. Instrument for potentiometric electrochemical measurements. U.S. Patent 4,851,104, July 25, 1989.
(16) Brown, G. C. Deep sea pH sensor. U.S. Patent 8,828,207, September 9, 2014.
(17) Ross, J. W.; Frant, M. S.; Riseman, J. H. U.S. Patent 3,563,874, 1971.
(18) Rajbhandari, A.; Manandhar, K.; Pradhananga, R. R. *J. Nepal Chem. Soc.* **2012**, *30*, 168−173.
(19) Bergveld, P. *Sens. Actuators, B* **2003**, *88*, 1−20.
(20) Carter, B. R.; Radich, J. A.; Doyle, H. L.; Dickson, A. G. *Limnol. Oceanogr.: Methods* **2013**, *11*, 16−27.
(21) *Guide to best practices for ocean CO_2 measurements*; Dickson, A. G., Sabine, C. L., Christian, J. R., Eds.; PICES Special Publication 3: 2007; p 191.
(22) O'Sullivan, D. W.; Millero, F. J. *Mar. Chem.* **1998**, *60*, 75−83.
(23) Oelßner, W.; Zosel, J.; Guth, U.; Pechstein, T.; Babel, W.; Connery, J. G.; Demuth, C.; Grote Gansey, M.; Verburg, J. B. *Sens. Actuators, B* **2005**, *105*, 104−117.
(24) Takeshita, Y.; Martz, T. R.; Johnson, K. S.; Dickson, A. G. *Anal. Chem.* **2014**, *86*, 11189−11195.
(25) Harned, H. S.; Ehlers, R. W. *J. Am. Chem. Soc.* **1932**, *54*, 1350−1357.
(26) Millero, F. J. In *Chemical Oceanography*; Riley, J. P., Chester, R., Eds.; Academic Press: London, 1983; Vol. *8*, pp 1−88.
(27) Khoo, K. H.; Ramette, R. W.; Culberson, C. H.; Bates, R. G. *Anal. Chem.* **1977**, *49*, 29−34.
(28) Marion, G. M.; Millero, F. J.; Camões, M. F.; Spitzer, P.; Feistel, R.; Chen, C.-T. A. *Mar. Chem.* **2011**, *126*, 89−96.
(29) Lewis, E. L. *IEEE J. Oceanic Eng.* **1980**, *5*, 3−8.
(30) Dickson, A. G. *J. Chem. Thermodyn.* **1990**, *22*, 113−127.
(31) Millero, F. J. *Chem. Rev.* **2007**, *107*, 308−341.
(32) Waters, J. F.; Millero, F. J. *Mar. Chem.* **2013**, *149*, 8−22.
(33) Culberson, C.; Pytkowicz, R. M. *Limnol. Oceanogr.* **1968**, *13*, 403−417.
(34) Lewis, E.; Wallace, D. W. R. *Program Developed for CO_2 System Calculations*; ORNL/CDIAC-105; Carbon Dioxide Inf. Anal. Cent., Oak Ridge Natl. Lab.: Oak Ridge, TN, 1998; 38 pp.
(35) Feely, R. A.; Sabine, C. L.; Hernandez-Ayon, J. M.; Ianson, D.; Hales, B. *Science* **2008**, *320*, 1490−1492.
(36) Bresnahan, P. J., Jr.; Martz, T. R.; Takeshita, Y.; Johnson, K. S.; LaShomb, M. *Methods Oceanogr.* **2014**, *9*, 44−60.
(37) Johnson, K. S.; Coletti, L. J.; Jannasch, H. W.; Sakamoto, C. M.; Swift, D. D.; Riser, S. C. *J. Atmos. Oceanic Technol.* **2013**, *30*, 1854−1866.
(38) Juranek, L. W.; Feely, R. A.; Gilbert, D.; Freeland, H.; Miller, L. A. *Geophys. Res. Lett.* **2011**, *38*, L17603.
(39) Suzuki, T., Ishii, M.; Aoyama, M.; Christian, J. R.; Enyo, K.; Kawano, T.; Key, R. M.; Kosugi, N.; Kozyr, A.; Miller, L. A.; Murata, A.; Nakano, T.; Ono, T.; Saino, T.; Sasaki, K.; Sasano, D.; Takatani, Y.; Wakita, M.; Sabine, C. *PACIFICA Data Synthesis Project*; ORNL/CDIAC-159, NDP-092; Carbon Dioxide Information Analysis Center, Oak Ridge National Laboratory, U.S. Department of Energy: Oak Ridge, TN, 2013; doi:10.3334/CDIAC/OTG.PACIFICA_NDP092.
(40) Newton, J. A.; Feely, R. A.; Jewett, E. B.; Williamson, P.; Mathis, J. *Global Ocean Acidification Observing Network: Requirements and Governance Plan*, 2nd ed.; 2015. http://www.goa-on.org/docs/GOA-ON_plan_print.pdf (accessed Feb 1, 2016).

DOI: 10.1021/acs.analchem.5b04653
Anal. Chem. 2016, 88, 3249−3256